

# Chronic exposure to simulated space conditions predominantly affects cytoskeleton remodeling and oxidative stress response in mouse fetal fibroblasts

MICHAËL BECK<sup>1,2</sup>, MARJAN MOREELS<sup>1</sup>, ROEL QUINTENS<sup>1</sup>, KHALIL ABOU-EL-ARDAT<sup>1,2</sup>,  
HUSSEIN EL-SAGHIRE<sup>1,3</sup>, KEVIN TABURY<sup>1</sup>, ARLETTE MICHAUX<sup>1</sup>, ANN JANSSEN<sup>1</sup>, MIEKE NEEFS<sup>1</sup>,  
PATRICK VAN OOSTVELDT<sup>2,4</sup>, WINNOK H. DE VOS<sup>2,4,5</sup> and SARAH BAATOUT<sup>1,2</sup>

<sup>1</sup>Radiobiology Unit, Expert Group of Molecular and Cellular Biology, Institute for Environment, Health and Safety, Belgian Nuclear Research Centre (SCK-CEN), Mol; <sup>2</sup>Department of Molecular Biotechnology, <sup>3</sup>Department of Basic Medical Sciences, Faculty of Medicine and Health Sciences, <sup>4</sup>NB-Photonics, Ghent University, Ghent; <sup>5</sup>Laboratory of Cell Biology and Histology, Department of Veterinary Sciences, Antwerp University, Antwerp, Belgium

Received February 2, 2014; Accepted March 24, 2014

DOI: 10.3892/ijmm.2014.1785

**Abstract.** Microgravity and cosmic rays as found in space are difficult to recreate on earth. However, ground-based models exist to simulate space flight experiments. In the present study, an experimental model was utilized to monitor gene expression changes in fetal skin fibroblasts of murine origin. Cells were continuously subjected for 65 h to a low dose (55 mSv) of ionizing radiation (IR), comprising a mixture of high-linear energy transfer (LET) neutrons and low-LET gamma-rays, and/or simulated microgravity using the random positioning machine (RPM), after which microarrays were performed. The data were analyzed both by gene set enrichment analysis (GSEA) and single gene analysis (SGA). Simulated microgravity affected fetal murine fibroblasts by inducing oxidative stress responsive genes. Three of these genes are targets of the nuclear factor-erythroid 2 p45-related factor 2 (Nrf2), which may play a role in the cell response to simulated microgravity. In addition, simulated gravity decreased the expression of genes involved in cytoskeleton remodeling, which may have been caused by the downregulation of the serum response factor (SRF), possibly through the Rho signaling pathway. Similarly, chronic exposure to low-dose IR caused the downregulation of genes involved in cytoskeleton remodeling, as well as in cell cycle regulation and DNA damage response pathways. Many of

the genes or gene sets that were altered in the individual treatments (RPM or IR) were not altered in the combined treatment (RPM and IR), indicating a complex interaction between RPM and IR.

## Introduction

In the present study, we established an *in vitro* model in which primary cultures of fetal fibroblasts from murine origin (PFC) were subjected for 65 h to simulated microgravity, chronic irradiation or a combination. Genome-wide gene expression changes were thereafter assessed by microarrays. For microgravity simulation, we used the random positioning machine (RPM), which is one of the most widely used instruments for this purpose and has proven valuable in many cell types (1-6). As far as cosmic radiation is concerned, simulating the wide variety of ions ranging from low to very high energies encountered in space is problematic, particularly if irradiation is combined with microgravity simulation models. At present, no facility offers the possibility of producing chronic exposures of very high-energy beams consisting of multiple charged particles. We therefore used a source of californium Cf-252 for low-dose rate long-term exposure consisting of a mixture of high-linear energy transfer (LET) neutrons and low-LET gamma-rays (7).

The large amount of data generated with a high-throughput technology such as microarrays constitutes a double-edged sword: whole expression pattern may be recorded, but extracting the relevant information becomes more challenging (8,9). To overcome this problem, analysis tools have been developed, such as single gene statistical analysis methods (SGA), which are widely used to determine the differentially expressed genes, and the gene set enrichment analysis (GSEA), which aims to identify gene expression differences in groups of genes, for instance in those acting synergistically in a cell process (9,10). The two analytical methods were used concomitantly in this study.

---

*Correspondence to:* Professor Sarah Baatout, Radiobiology Unit, Expert Group of Molecular and Cellular Biology, Institute for Environment, Health and Safety, Belgian Nuclear Research Centre (SCK-CEN), Boeretang 200, B-2400 Mol, Belgium  
E-mail: sarah.baatout@sckcen.be

*Key words:* simulated space conditions, microarrays, cytoskeleton, oxidative stress, DNA damage

## Materials and methods

**Cell culture.** All the animals were handled following the Belgian legislation after approval by the appropriate Ethics Committees (agreement number 08-002). BALB/cJ Rj (Janvier Laboratories, Saint-Berthevin, France) fetuses (three males and three females) originating from two different litters were dissected 17 days post-conception (day 0 being the fertilization day). Their skin was harvested and mechanically dissociated. The obtained tissue was enzymatically digested for 1 h at 37°C in phosphate-buffered saline (PBS; N.V. Invitrogen SA, Merelbeke, Belgium) solution containing 1 mg/ml of collagenase/dispase (Roche, Mannheim, Germany) and 5 mg/ml of trypsin 2,000 E/g (Merck KGaA, Darmstadt, Germany). The enzymatic reaction was subsequently stopped by adding fetal bovine serum (FBS; N.V. Invitrogen SA). The obtained cell suspension was subsequently centrifuged for 10 min at 350 x g and the cells were seeded in 6-well plates in F12 medium supplemented with 20% FBS and 1% penicillin/streptomycin (both from N.V. Invitrogen SA), one fetus skin in each well. The cells were allowed to grow for up to 3 or 4 passages at 37°C (5%, CO<sub>2</sub>) and were subsequently frozen in FBS with 10% dimethyl sulfoxide (Sigma-Aldrich, St. Louis, MO, USA). The primary cultures were then thawed and allowed to grow for two weeks. The cells were seeded at a density of  $\times 10^5$  cells in 12.5 cm<sup>2</sup> flasks and allowed to adhere for 24 h prior to treatment.

**Simulation of space conditions.** Exposure to simulated space conditions included microgravity simulation using the desktop RPM (Dutch Space, Leiden, The Netherlands) and ionizing radiation (IR) (7). The exposure lasted for a period of 65 h. Four treatment conditions were used: controls (CTRL), microgravity simulation (RPM), irradiation and a combination of the treatment methods (RPM and IR). For microgravity simulation, the flasks were completely filled with medium, sealed and placed on the RPM at a rotational velocity between 55 and 65°/sec. Direction, speed and interval were set as random. The CTRL were placed in the same incubator under the same conditions as the treated samples. For chronic low-dose irradiation, the cells were exposed to a mixture of neutrons (98.2%) and gamma-rays (1.8%) directly or indirectly originating from a Cf-252 source were placed at 4.13 m from the incubator. The dosimetry was performed with bubble detectors as previously described (11) for neutron irradiation and with 600 cc ionization chamber (NE) coupled with a Farmer electrometer for gamma-rays. The total dose received was  $55.94 \pm 19.70$  mSv ( $862 \mu\text{Sv/h}$ ), which approximately corresponds to 35 times the dose rate measured on the International Space Station (ISS) (12), the total dose corresponding approximately to a stay of 100 days in the ISS.

**RNA extraction.** Immediately after treatment, adherent cells were washed in PBS, lysed in 350 ml of AllPrep DNA/RNA/Protein Mini kit lysis buffer (Qiagen, Hilden, Germany) and frozen at -80°C. RNA was extracted using the same kit and its concentration was measured using the Nanodrop spectrophotometer (Thermo Scientific, Waltham, MA, USA) while its quality (RNA integrity number, RIN) was determined with Agilent's lab-on-chip Bioanalyzer 2100

(Agilent Technologies, Inc., Palo Alto, CA, USA). All the RNA samples had a RIN value of  $>9.0$ .

**Affymetrix microarrays and data analysis.** The RNA was treated using the GeneChip WT cDNA Synthesis and Amplification kit (Affymetrix, Santa Clara, CA, USA) according to the manufacturer's instructions. The resulting RNA was hybridized onto Affymetrix Mouse Gene 1.0 ST arrays.

Raw data (.cel-files) were imported at exon level in Partek Genomics Suite v6.5 (Partek Incorporated, St. Louis, MO, USA). Briefly, robust Multi-array Average (RMA) background correction was applied, data were normalized by quantile normalization and probe set summarization was performed using the median polish method. Gene summarization was performed using One-Step Tukey's Biweight method. These data were further analyzed with the Partek Genomics Suite software for SGA and by the GSEA software (v2.0, Broad Institute of Harvard and MIT, Cambridge, MA, USA).

For the single gene method, taking into consideration the scan date (also available for the litter), the fetus, the gender and the treatment as factors, a four-way ANOVA was performed to determine the genes that had a significantly altered expression for different conditions. For the pathway analysis, KEGG and PathArt databases were analyzed with ArrayTrack v3.3.0 (National Center for Toxicological Research, Jefferson, AR, USA).

For the GSEA, a selection of 144 gene sets from gene ontology (GO) databases was based on biological relevance (Table I). Gene sets were considered to be significantly differently regulated with a false discovery rate (FDR) when  $q < 0.05$ .

## Results

Single gene analysis revealed that 119 genes were down-regulated and 55 genes were upregulated by  $>1.5$ -fold change (unadjusted p-value  $< 0.01$ ) across all the treatments (Fig. 1 and an exhaustive list of the differentially expressed genes can be found in Table II). KEGG and PathArt databases indicated that the 54 genes that were downregulated only by RPM treatment were mostly involved in cell cycle regulation (p53- and p21-mediated pathways), in cytoskeleton modeling, cell junctions and cell signaling via integrins, IL-1, and TGF- $\beta$ . Within the list of individual genes that were downregulated after IR or RPM and IR treatments, no clear pathway was found. On the other hand, in the 52 genes that were upregulated following RPM and RPM and IR treatments, interleukin signaling (IL-11 and MMP) and glutathione metabolism were the most prominent pathways affected. Some genes were differentially expressed by RPM and RPM and IR, however, only a few genes were common between IR and RPM and IR. Six genes were upregulated (Slp3, Rab11b, Ptger3, Vldlr, Cnn1 and Serping1) and only one predicted gene of unknown function was downregulated (Gm13668) in both irradiated treatments (IR and RPM and IR). The upregulated genes were mostly membrane proteins, G-protein coupled (Slp3 and Ptger3) or involved in ligand endocytosis (Rab11b and Vldlr). Cnn1 and Serping1, involved in cytoskeleton organization and peptidase inhibition, respectively, were both upregulated in all the treatments, including RPM.

Table I. List of the 144 gene sets selected for GSEA.

Gene set description	Gene Ontology
Actin binding	GO:0003779
Actin cytoskeleton	GO:0015629
Activation of JNK activity	GO:0007257
Activation of MAPK activity	GO:0000187
Adherens junction	GO:0005912
Anti-apoptosis	GO:0006916
Antioxidant activity	GO:0016209
Apoptosis GO	GO:0006915
Base excision repair	GO:0006284
Calcium ion binding	GO:0005509
Calcium ion transport	GO:0006816
Caspase activation	GO:0006919
Cell-cell adhesion	GO:0016337
Cell-cell signaling	GO:0007267
Cell cycle arrest	GO:0007050
Cell cycle	GO:0007049
Cell cycle process	GO:0022402
Cell junction	GO:0030054
Cell matrix adhesion	GO:0007160
Cellular respiration	GO:0045333
Centrosome	GO:0005813
Chaperone binding	GO:0051087
Chromatin	GO:0000785
Chromosome	GO:0005694
Collagen	GO:0005581
Cortical cytoskeleton	GO:0030863
Cytokine activity	GO:0005125
Cytoskeletal protein binding	GO:0008092
Cytoskeleton	GO:0005856
DNA damage checkpoint	GO:0000077
DNA integrity checkpoint	GO:0031570
DNA repair	GO:0006281
Double-strand break repair	GO:0006302
Electron transport	GO:0006118
Embryonic development	GO:0009790
Endoplasmic reticulum	GO:0005783
Excretion	GO:0007588
Extracellular matrix	GO:0031012
Focal adhesion	GO:0005925
G-protein coupled receptor activity	GO:0004930
G-protein coupled receptor protein signaling pathway	GO:0007186
G-protein signaling coupled to IP3 second messenger phospholipase C activating	GO:0007200
G1 phase	GO:0051318
G1/S transition of mitotic cell cycle	GO:0000082
G2/M transition of mitotic cell cycle	GO:0000086
Glutathione transferase activity	GO:0004364
Golgi apparatus	GO:0005794
GTPase regulator activity	GO:0030695
Histone modification	GO:0016570
Hormone activity	GO:0005179

Table I. Continued.

Gene set description	Gene Ontology
Inositol or phosphatidylinositol kinase activity	GO:0004428
Inositol or phosphatidylinositol phosphatase activity	GO:0004437
Inositol or phosphatidylinositol phosphodiesterase activity	GO:0004434
Insulin receptor signaling pathway	GO:0008286
Integrin binding	GO:0005178
Intercellular junction	GO:0005911
Ion channel activity	GO:0005216
JAK/STAT cascade	GO:0007259
JNK cascade	GO:0007254
Lamellipodium	GO:0030027
Lipid binding	GO:0008289
M phase	GO:0000279
Magnesium ion binding	GO:0000287
MAP kinase activity	GO:0004707
MAPKKK cascade	GO:0000165
Microtubule	GO:0005874
Microtubule cytoskeleton	GO:0015630
Mitochondrial inner membrane	GO:0005743
Mitochondrial respiratory chain	GO:0005746
Mitochondrion	GO:0005739
Motor activity	GO:0003774
Negative regulation of apoptosis	GO:0043066
Negative regulation of cell adhesion	GO:0007162
Negative regulation of cell cycle	GO:0045786
Negative regulation of cell proliferation	GO:0008285
Negative regulation of cellular metabolic process	GO:0031324
Negative regulation of signal transduction	GO:0009968
Negative regulation of transcription	GO:0016481
Negative regulation of translation	GO:0017148
Nuclear pore	GO:0005643
Nucleolus	GO:0005730
Nucleus	GO:0005634
Oligosaccharide metabolic process	GO:0009311
Phosphoinositide-mediated signaling	GO:0048015
Phospholipase activity	GO:0004620
Phospholipid binding	GO:0005543
Phosphorylation	GO:0016310
Positive regulation of caspase activity	GO:0043280
Positive regulation of cell adhesion	GO:0045785
Positive regulation of cell cycle	GO:0045787
Positive regulation of cell proliferation	GO:0008284
Positive regulation of JNK activity	GO:0043507
Positive regulation of MAP kinase activity	GO:0043406
Positive regulation of protein metabolic process	GO:0051247
Positive regulation of signal transduction	GO:0009967
Positive regulation of transcription	GO:0045941
Positive regulation of translation	GO:0045727

Table I. Continued.

Gene set description	Gene Ontology
Post-translational protein modification	GO:0043687
Potassium ion transport	GO:0006813
Programmed cell death	GO:0012501
Protein folding	GO:0006457
Protein kinase activity	GO:0004672
Protein kinase cascade	GO:0007243
Protein metabolic process	GO:0019538
Protein modification process	GO:0006464
Protein/RNA complex assembly	GO:0022618
Protein serine/threonine kinase activity	GO:0004674
Protein ubiquitination	GO:0016567
Proteolysis	GO:0006508
RAS GTPase activator activity	GO:0005099
RAS GTPase binding	GO:0017016
Receptor binding	GO:0005102
Regulation of apoptosis	GO:0042981
Replication fork	GO:0005657
Respiratory chain complex I	GO:0045271
Response to DNA damage stimulus	GO:0006974
Response to ionizing radiation	GO:0010212
Response to radiation	GO:0009314
Response to stress	GO:0006950
RHO GTPase activator activity	GO:0005100
RHO protein signal transduction	GO:0007266
Rhodopsin-like receptor activity	GO:0001584
RNA helicase activity	GO:0003724
RNA processing	GO:0006396
RNA splicing	GO:0008380
Ruffle	GO:0001726
S phase	GO:0051320
Second messenger-mediated signaling	GO:0019932
Small conjugated protein ligase activity	GO:0019787
Small GTPase-mediated signal transduction	GO:0007264
Sodium channel activity	GO:0005272
Spindle	GO:0005819
Spliceosome	GO:0005681
Structural constituent of cytoskeleton	GO:0005200
Structural constituent of ribosome	GO:0003735
Tight junction	GO:0005923
Transcription	GO:0006350
Translation	GO:0006412
Transmembrane receptor protein kinase activity	GO:0019199
Transmembrane transporter activity	GO:0022857
T-RNA metabolic process	GO:0006399
Ubiquitin cycle	GO:0006512
Ubiquitin protein ligase activity	GO:0004842
Voltage-gated channel activity	GO:0022832

GSEA, gene set enrichment analysis.

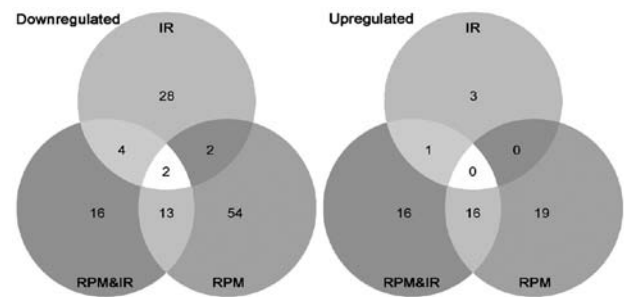


Figure 1. Venn diagram showing the number of downregulated (left) or upregulated (right) genes in murine fetal fibroblasts following one of the three space simulation treatments ( $p < 0.01$ , fold change  $> 1.5$ ): chronic exposure to low dose of ionizing radiation (IR), simulated microgravity (RPM) or a combination of RPM and IR.

In contrast to the results obtained by SGA, GSEA revealed a high impact of IR on coordinately differentially expressed genes. A total of 63 gene sets were significantly downregulated following chronic low-dose irradiation. Of the 63 genes, 30 were exclusively enriched in irradiated samples (Fig. 2), although this number may be an overestimation due to redundancy between some of the gene sets. The gene sets that were specifically downregulated after irradiation conditions are mostly involved in DNA damage response, cell signaling, cell cycle, RNA processing and protein turnover (Table III). Moreover, we detected significantly downregulated gene sets involved in cell signaling, cell cycle, transcription, protein turnover, cell shape, adhesion, motility and communication for all the treatments. Of note, two gene sets involved in oxidative phosphorylation were significantly downregulated solely in the RPM and IR samples. No gene set was significantly upregulated in any of the treatments.

## Discussion

In this study, primary cultures of murine fetal fibroblasts were chronically exposed (65 h) to simulated space conditions including simulated microgravity via RPM and a low-dose mixture of neutrons and gamma-rays (IR). The duration of the experiment was chosen to allow cellular adaptation to the simulated microgravity environment for instance for cytoskeleton remodeling (13,14), in order to decrease the primary stress response mechanisms and to better characterize the effects of chronic exposure to these conditions. Microarrays were performed on RNA harvested from CTRL, IR, RPM and RPM and IR conditions. Microarrays generate a substantial amount of information on the gene expression pattern of cells subjected to a defined treatment. However, a  $< 2$ -fold difference in the gene expression is often not sufficient to meet the requirements for statistical significance (8). Identification of moderate gene expression differences in groups of genes acting together in a cell process can nevertheless be achieved by means of GSEA. For this reason, we analyzed our microarray output data using the single gene analysis method as well as GSEA.

*The RPM has a dominant impact on single gene expression.* The SGA method revealed a significant impact of 65 h of simulated microgravity on gene expression in murine fetal fibroblasts. The combination of RPM and IR triggered a

**Table II. Down- and upregulated genes following IR, RPM or RPM and IR treatments (p<0.001, fold change >1.5).**
**A, Down- and upregulated genes following IR**

Gene symbol	GenBank	p-value	FC
Rab11b	NM_008997	5,48E-03	-2,026
Csgalnact1	NM_172753	9,04E-03	-1,989
Smarca5	NM_053124	4,08E-03	-1,986
Tceb3	NM_013736	6,85E-03	-1,953
Serping1	NM_009776	1,39E-03	-1,948
Ppp1r2	NM_025800	9,20E-03	-1,801
Ptgfrn	NM_011197	4,38E-03	-1,801
Dnaja1	NM_008298	6,13E-03	-1,772
Arhgap24	NM_029270	6,13E-03	-1,767
Thra	NM_178060	3,67E-04	-1,728
Itga8	NM_001001309	9,74E-03	-1,718
Gpr108	NM_030084	2,40E-03	-1,696
Zfp346	NM_012017	1,54E-04	-1,672
Rbmx	NM_011252	1,04E-03	-1,655
B4galt6	NM_019737	9,25E-03	-1,638
BC003331	NM_145511	5,04E-03	-1,637
Vldlr	NM_013703	3,68E-03	-1,636
Unc93b1	NM_019449	5,57E-04	-1,625
Pip4k2a	NM_008845	3,79E-04	-1,622
Mgll	NM_001166251	2,52E-03	-1,620
BC005624	NM_144885	2,10E-03	-1,619
S1pr3	NM_010101	2,64E-03	-1,613
Prkcd	NM_011103	3,32E-03	-1,583
Cnn1	NM_009922	4,26E-03	-1,575
P2ry2	NM_008773	6,80E-03	-1,566
Saps1	NM_172894	8,65E-03	-1,566
Casc4	NM_177054	4,45E-03	-1,559
Opal	NM_133752	7,47E-03	-1,552
Emb	NM_010330	5,84E-04	-1,551
Cyb5d1	NM_001045525	5,23E-03	-1,549
Ptger3	NM_011196	1,41E-03	-1,549
Usp30	NM_001033202	1,36E-03	-1,543
Tbc1d2b	NM_194334	6,00E-03	-1,539
Cyld	NM_001128169	2,57E-03	-1,530
Trip4	NM_019797	8,21E-03	-1,520
Luzp1	NM_024452	9,75E-03	-1,502
Gm13668	XR_032757	6,87E-04	1,856
Hist1h2ao	NM_001177544	3,69E-03	1,710
Bmyc	NM_023326	3,25E-03	1,575
4930458L03Rik	NM_030047	1,32E-03	1,523

**B, Down- and upregulated genes following RPM**

Gene symbol	GenBank	p-value	FC
Dmpk	NM_032418	2,73E-05	-2,522
Myh10	NM_175260	1,51E-03	-2,485
Myh9	NM_022410	2,08E-03	-2,432
Maob	NM_172778	1,48E-04	-2,335
Slc38a4	NM_027052	9,81E-04	-2,270
Cnn1	NM_009922	4,53E-05	-2,147
Adhl	NM_007409	2,01E-04	-2,126
Serping1	NM_009776	5,85E-04	-2,095

**Table II. Continued.**

Gene symbol	GenBank	p-value	FC
Actg2	NM_009610	3,08E-05	-2,089
Ccnb2	NM_007630	2,94E-04	-2,071
Kif20a	NM_001166406	1,35E-04	-2,023
Gjb2	NM_008125	1,16E-04	-2,014
Anln	NM_028390	8,66E-04	-2,001
Nfix	NM_001081981	3,95E-03	-1,964
Itga8	NM_001001309	2,19E-03	-1,963
Pygb	NM_153781	1,46E-03	-1,913
Bub1	NM_001113179	3,71E-05	-1,881
Ly6c1	NM_010741	9,89E-04	-1,879
ND4L	ENSMUST00000084013	2,03E-05	-1,843
Myl9	NM_172118	1,95E-04	-1,830
Actn4	NM_021895	8,48E-03	-1,819
Itgb11	NM_145467	8,49E-03	-1,814
Efemp1	NM_146015	6,17E-04	-1,801
D17H6S56E-5	L78788	2,29E-07	-1,791
Plk1	NM_011121	1,55E-03	-1,774
ND4L	ENSMUST00000084013	3,76E-05	-1,750
Susd2	NM_027890	2,62E-04	-1,736
Ly6c2	NM_001099217	7,26E-04	-1,731
Ucp2	NM_011671	4,37E-04	-1,717
Cenpa	NM_007681	3,25E-03	-1,713
Nuf2	NM_023284	6,69E-04	-1,711
Rbmx	NM_011252	7,19E-04	-1,692
Kif2c	NM_134471	2,28E-03	-1,687
Rpl22l1	NM_026517	9,88E-03	-1,678
Ly6a	NM_010738	8,47E-03	-1,671
Pkp2	NM_026163	1,21E-04	-1,667
Tgfb1i1	NM_009365	6,54E-03	-1,652
Acta1	NM_009606	7,19E-06	-1,644
Gas2l3	NM_001033331	5,26E-04	-1,643
Lrrc17	NM_028977	4,37E-03	-1,642
2810417H13Rik	NM_026515	3,58E-03	-1,640
Lpar4	NM_175271	3,20E-03	-1,639
Dlgap5	NM_144553	1,76E-03	-1,622
Hgf	NM_010427	1,71E-03	-1,611
Trp53inp2	NM_178111	1,30E-03	-1,605
Cyb5r3	NM_029787	1,06E-03	-1,603
Mfap2	NM_008546	6,77E-04	-1,600
Cyp1b1	NM_009994	5,70E-03	-1,597
Trpv2	NM_011706	4,75E-03	-1,596
Kif23	NM_024245	1,56E-03	-1,591
Sh3pxd2a	NM_008018	1,37E-03	-1,566
ND2	ENSMUST00000082396	1,35E-03	-1,564
Tgfb3	NM_009368	1,15E-03	-1,562
Scd2	NM_009128	5,24E-03	-1,554
Dner	NM_152915	1,80E-03	-1,546
Pdgfrl	NM_026840	4,88E-04	-1,543
Cenpm	NM_025639	6,47E-03	-1,539
Ppp1r3c	NM_016854	1,04E-03	-1,536
Fam114a1	NM_026667	1,68E-03	-1,533
D2Ertd750e	NM_026412	7,48E-04	-1,533
Nkd2	NM_028186	7,87E-03	-1,531

Table II. Continued.

Gene symbol	GenBank	p-value	FC
Nov	NM_010930	9,41E-03	-1,529
Tgm2	NM_009373	2,62E-03	-1,525
Nucb2	NM_001130479	7,36E-03	-1,518
5730469M10Rik	BC056635	1,03E-03	-1,516
Ccna2	NM_009828	8,65E-03	-1,514
Maged2	NM_030700	6,56E-03	-1,512
Eif4b	NM_145625	7,83E-03	-1,512
Sepx1	NM_013759	2,65E-04	-1,506
Shisa4	NM_175259	5,60E-03	-1,503
St3gal5	NM_011375	8,29E-03	-1,502
Fhl5	NM_021318	2,32E-04	-1,502
Serpib9e	NM_011456	2,02E-03	2,514
Gsta1	NM_008181	1,59E-05	2,232
Taf1d	BC056964	1,32E-03	2,223
Gsta1	NM_008181	2,15E-05	2,210
Prl2c3	NM_011118	2,70E-05	2,209
Snhg1	AK051045	5,45E-06	2,192
Prl2c5	NM_181852	2,79E-04	2,179
Malat1	NR_002847	1,90E-04	2,139
Il1r1	NM_001025602	2,81E-04	2,061
Snhg1	AK051045	1,78E-05	1,967
Gm10639	NM_001122660	2,00E-04	1,908
Sema7a	NM_011352	5,57E-04	1,870
Lce1h	NM_026335	6,44E-03	1,841
Taf1d	BC056964	7,18E-04	1,812
Crcr1	NM_028798	3,49E-04	1,802
Gm8074	XM_983501	3,90E-04	1,799
Lsm1	NM_026032	1,31E-03	1,794
2310002L13Rik	ENSMUST00000025390	4,85E-04	1,771
Sirt7	NM_153056	4,15E-04	1,760
Serpib9b	NM_011452	4,07E-06	1,734
Snord14e	NR_028275	7,22E-04	1,704
Gsta2	NM_008182	7,50E-07	1,700
Ppbbp	NM_023785	5,04E-03	1,691
Hsd3b6	NM_013821	1,21E-04	1,684
Snord14d	NR_028274	7,27E-04	1,679
Hmox1	NM_010442	5,24E-06	1,678
Clef1	NM_019952	1,97E-04	1,671
Snord14d	NR_028274	7,39E-04	1,667
Procr	NM_011171	2,00E-03	1,649
Hist1h4i	NM_175656	4,77E-03	1,635
Dusp4	NM_176933	4,07E-03	1,626
Mmp10	NM_019471	6,51E-04	1,587
Cops3	NM_011991	1,24E-03	1,584
Gas5	NR_002840	3,87E-03	1,573
Chrna1	NM_007389	1,19E-03	1,565
Ifrd1	NM_013562	1,44E-03	1,556
D4Wsu53e	BC043057	2,60E-03	1,515
S100a7a	NM_199422	8,26E-03	1,513
Scarna17	NR_028560	6,25E-04	1,512
Scarna17	NR_028560	6,25E-04	1,512

Table II. Continued.

C, Down- and upregulated genes following RPM and IR			
Gene symbol	GenBank	p-value	FC
Cnn1	NM_009922	6,32E-06	-2,494
Serping1	NM_009776	1,65E-04	-2,337
Dmpk	NM_032418	1,36E-04	-2,206
Actg2	NM_009610	1,44E-05	-2,203
Adh1	NM_007409	2,24E-04	-2,107
Rab11b	NM_008997	4,88E-03	-2,051
Itgbl1	NM_145467	2,48E-03	-2,041
Gjb2	NM_008125	1,20E-04	-2,009
Srpx	NM_016911	1,74E-05	-1,882
Myl9	NM_172118	1,72E-04	-1,844
S1pr3	NM_010101	4,04E-04	-1,824
Maob	NM_172778	2,99E-03	-1,814
Tmem45a	NM_019631	3,16E-04	-1,793
Pdgfr1	NM_026840	3,28E-05	-1,772
Nov	NM_010930	1,36E-03	-1,749
Pigc	NM_026078	5,96E-03	-1,691
Il1r1	NM_008362	5,64E-03	-1,690
Vldlr	NM_013703	2,37E-03	-1,687
Susd2	NM_027890	6,17E-04	-1,652
Ptger3	NM_011196	4,43E-04	-1,651
Lysmd3	NM_030257	2,93E-03	-1,650
Fhl1	NM_001077361	1,90E-08	-1,629
Cyp1b1	NM_009994	4,48E-03	-1,625
Plk1	NM_011121	6,41E-03	-1,600
St3gal5	NM_011375	3,71E-03	-1,583
Rab13	NM_026677	7,09E-04	-1,581
Snta1	NM_009228	4,11E-05	-1,577
Aqp1	NM_007472	5,14E-03	-1,556
Cpa6	NM_177834	4,01E-03	-1,554
Nosip	NM_025533	1,35E-03	-1,540
Pla2g16	NM_139269	5,13E-03	-1,532
Lmod1	NM_053106	3,01E-03	-1,523
Zcchc17	NM_153160	4,13E-03	-1,519
Islr	NM_012043	1,27E-03	-1,509
6330406I15Rik	BC116246	1,22E-04	-1,502
Serpib9e	NM_011456	7,91E-04	2,818
Slc40a1	NM_016917	1,83E-05	2,670
Taf1d	BC056964	2,85E-04	2,595
Snhg1	AK051045	8,57E-06	2,126
Prl2c3	NM_011118	8,34E-05	2,037
Gsta1	NM_008181	1,21E-04	1,938
Procr	NM_011171	1,83E-04	1,935
Gsta1	NM_008181	1,60E-04	1,921
Mmp13	NM_008607	5,88E-04	1,894
Malat1	NR_002847	1,05E-03	1,873
Serpib9g	NM_011455	5,62E-03	1,865
Snhg1	AK051045	5,03E-05	1,848
Serpib9g	NM_011455	5,24E-03	1,801
310002L13Rik	ENSMUST00000025390	4,28E-04	1,785
Gm8074	XM_983501	6,00E-04	1,750
Myc	NM_010849	1,98E-05	1,748

Table II. Continued.

Gene symbol	GenBank	p-value	FC
Peg10	NM_130877	1,83E-03	1,746
Mamdc2	NM_174857	7,44E-04	1,744
I111	NM_008350	9,82E-03	1,728
Mmp3	NM_010809	8,35E-03	1,724
Fabp7	NM_021272	2,79E-03	1,693
Serpib9b	NM_011452	7,99E-06	1,681
Taf1d	BC056964	2,40E-03	1,667
Gmn	AF068780	7,71E-03	1,620
Gm10639	NM_001122660	2,64E-03	1,610
Dusp4	NM_176933	5,31E-03	1,596
Bcl2l11	NM_207680	9,00E-03	1,595
Ctu1	NM_145582	1,01E-03	1,594
Gsta2	NM_008182	3,74E-06	1,591
Hsd3b6	NM_013821	5,25E-04	1,561
Gm13668	XR_032757	8,44E-03	1,553
Ang2	NM_007449	1,54E-03	1,548
Scarna17	NR_028560	3,97E-04	1,545
Scarna17	NR_028560	3,97E-04	1,545
Hmox1	NM_010442	3,84E-05	1,541
Serpib9f	NM_183197	9,11E-04	1,540
Opa3	NM_207525	1,23E-03	1,540
Ormdl3	NM_025661	8,94E-03	1,505

IR, ionizing radiation; RPM, random positioning machine.

only a few genes were commonly differentially expressed in all irradiated treatments (IR and RPM and IR), of which there were only six known genes, all upregulated (S1p3, Rab11b, Ptger3, Vldlr, Cnn1 and Serping1), with most of them being involved in cell signaling. No explanation can be provided for the fact that few genes were commonly up- or downregulated in the irradiated treatments (with or without RPM). However the strong effect of RPM may have concealed a more subtle effect of IR, making it statistically less significant.

Among the upregulated genes following RPM treatment, glutathione-S-transferases  $\alpha$  1 and 2 (*Gsta1* and *Gsta2*) were prominent enzymes for the detoxification of breakdown products of oxidative stress (15). However, since the Affymetrix arrays cannot distinguish between the two isoforms due to their very high sequence homology (97%), we cannot dismiss the possibility that only one of the two isoforms was actually affected by the treatment. The modifier subunit of glutathione-cysteine ligase (*Gclm*) was significantly upregulated as well. The protein encoded by this gene was shown to play an important role in controlling the rate of glutathione synthesis in murine fetal fibroblasts (16). We also report upregulation of the heme oxygenase 1 (*Hmox1*), a cytoprotective enzyme against oxidative stress (17). In murine fibroblasts, its upregulation by curcumin was found to block radiation-induced reactive oxygen species (ROS) generation (18). Notably, these three genes are targets of the nuclear factor-erythroid 2 p45-related factor 2 (Nrf2) which induces transcription of cytoprotective genes containing antioxidant response elements (19). The transcription factor Nrf2 may therefore play a cytoprotective role against a possible oxidative stress induced by the RPM, which is in line with previous observations of increased oxidative stress in simulated microgravity (20-22).

After RPM treatment, two members of the actin filament family, *Actg2* and *Acta1* were downregulated. These genes were described in smooth (23) or skeletal muscles (24), respectively. Calponin 1 (*Cnn1*), a gene coding for a protein involved in the cytoskeleton organization (25), and four and a half LIM domains 1 (*Fhl1*), which functions in adherens junctions signaling to the cytoskeleton (26), were also downregulated. Notably, the four genes were shown to be regulated by the serum response factor (SRF). SRF was shown to be mediated by the Rho signaling pathway (25-27), which may have been triggered by the RPM. Rho signaling is believed to be an important pathway for focal adhesion assembly and cytoskeleton remodeling in response to cellular tension stress (28) and has been suggested to play a role in the microgravity response (21,29-31). Furthermore, Rho GTPase activities were shown to be increased in dermal fibroblasts subjected to simulated microgravity for 30 and 120 min, thereafter decreasing to reach similar values to those of the CTRL at 48 h of treatment (32). Our hypothesis is that a 65-h exposure to RPM induced downregulation of the Rho signaling pathway, which decreased the activity of the transcription factor SRF, decreasing in turn the expression of genes involved in cytoskeleton organization (*Cnn1*) and adherens junctions (*Fhl1*).

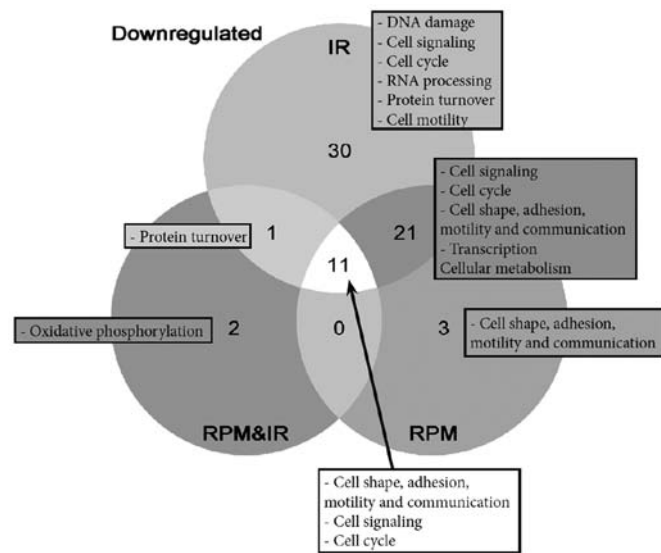


Figure 2. Venn diagram showing the number of gene sets significantly downregulated in murine fetal fibroblasts following one of the three space simulation treatments: chronic exposure to a low dose of irradiation (IR), simulated microgravity (RPM) or a combination of RPM and IR. Boxes include the cellular pathways in which these gene sets are involved.

differential expression of fewer genes than RPM alone. Only a few genes had an altered expression in IR samples, suggesting that such a low dose of radiation exerted a moderate impact on the expression of individual genes. It was also noted that

*IR has a dominant effect on gene sets.* At the gene set level, GSEA did not detect any upregulation, except for the structural constituents of the ribosome in IR-treated samples. This result is noteworthy as it did not occur with SGA. Since

Table III. Downregulated gene sets revealed by GSEA, based on the list of gene sets provided by Fig. 2.

Treatment	Cell process	Gene set (GO)	
IR	DNA damage	DNA damage checkpoint	
		DNA repair	
		Histone modification	
		Response to DNA damage stimulus	
		Response to radiation	
	Cell signaling	Response to stress	
		Negative regulation of signal transduction	
		Inositol or phosphatidylinositol kinase activity	
		Ras GTPase binding	
		Positive regulation of JNK activity	
		RHO GTPase activator activity	
		Protein kinase cascade	
		Magnesium ion binding	
		Protein serine/threonine kinase activity	
		Phosphorylation	
	Cell cycle	Cell cycle arrest (GO 0007050)	
		Negative regulation of cell cycle	
	RNA processing	RNA processing	
		RNA splicing	
Spliceosome			
Nuclear pore			
Protein turnover	tRNA metabolic process		
	Post translational protein modification		
	Endoplasmic reticulum		
	Golgi apparatus		
	Protein ubiquitination		
	Ubiquitin cycle		
	Ubiquitin protein ligase activity		
	Small conjugating protein ligase activity		
	Lamellipodium		
	Cell motility		
IR + RPM	Cell signaling	G protein signaling coupled to IP3	
		Phosphoinositide-mediated signaling	
		RAS GTPase activator activity	
		GTPase regulator activity	
		Small GTPase-mediated signal transduction	
		Transmembrane receptor	
		protein kinase activity	
		Protein kinase activity	
		Cell cycle	Cell cycle (GO 0007049)
		Centrosome	
	Cell shape, adhesion, motility and communication	Microtubule	
		Cytoskeletal protein binding	
		Ruffle	
		Cell junction	
		Collagen	
	Transcription	Extracellular matrix	
		Positive regulation of transcription	
		Negative regulation of transcription	
		RNA helicase activity	
Chromosome			
Cellular metabolism	Nucleolus		
	Negative regulation of cellular metabolic process		

Table III. Continued.

Treatment	Cell process	Gene set (GO)
IR + RPMIR + RPM and IR	Protein turnover	Protein/RNA complex assembly
IR + RPM + RPM + IR	Cell shape, adhesion, motility and communication	Cytoskeleton Actin binding Actin cytoskeleton Adherens junction Cell matrix adhesion Motor activity Microtubule cytoskeleton
	Cell signaling	Insulin receptor signaling pathway
	Cell cycle	Cell cycle process M phase Spindle
RPM	Cell shape, adhesion, motility and communication	Structural constituent of cytoskeleton Integrin binding Receptor binding
RPM + IR	Oxidative phosphorylation	Electron transport (GO 0006118) Mitochondrion

'+' shows the gene sets commonly differentially expressed between the treatments cited; IR, ionizing radiation; RPM, random positioning machine.

SGA and GSEA are purely statistical methods, it is unlikely that this result originates from an experimental issue, which may have affected both methods. We also examined the gene set selection, however, a screening of all the gene sets of GO provided the same result. Since the experimental design involved long-term irradiation, it is possible that a feedback loop occurred and decreased the expression pattern of the gene sets.

We identified a significant downregulation of 63 gene sets in response to low-dose IR, although single gene analysis did not reveal any important effects. Of the 63 gene sets, 30 were specifically enriched in IR-treated samples (Fig. 2). These latter gene sets are involved in DNA damage response, cell signaling, cell cycle, RNA processing, protein turnover or cell motility. Of note, the DNA damage response gene sets were downregulated, which may be explained by the long duration of continuous irradiation at an extremely slow-dose rate. It is possible that an adaptation mechanism of the cells to irradiation triggered a feedback loop to decrease the expression of these pathways, as was observed at the gene level (SGA) for SRF responsive genes in response to the RPM. Various other gene sets involved in the same cell processes were also enriched in the RPM, and RPM and IR treatments.

Many of the downregulated gene sets are involved in cell signaling, including Rho and Ras GTPases, inositol and phosphatidylinositol, JNK and insulin receptor-mediated pathways. The downregulation of these signaling pathways may lead to an alteration of the cell cycle (33). In addition to its major role in the cell response to radiation (34,35), the regulation of the cell cycle has been shown to be affected by simulated microgravity (36). GSEA revealed that gene sets involved in the positive regulation of the cell cycle were downregulated in all treatments. However, cells that were

only irradiated exhibited a significant downregulation of gene sets involved in cell cycle arrest, indicating no trend towards a pro- or anti-proliferative expression profile, while both RPM and RPM and IR showed an anti-proliferative expression profile. We suggest that all the treatments may have induced a general stress response that decreased the expression of cell cycle progression pathways, while irradiation alone also reduced the expression of genes involved in cell cycle arrest. This hypothesis is in agreement with the decreased expression of DNA damage response pathways that we also detected. In RPM and IR, the effect of the RPM may have concealed the cell cycle arrest gene set downregulation.

In addition, many gene sets involved in the composition of the cytoskeleton (actin and microtubule) and inter- (cell junctions) and extracellular connections (extracellular matrix) were affected by all the treatments. While it has been shown in various cell types that cytoskeleton remodeling starts immediately after exposure to simulated or real microgravity (21,29-31), few studies investigated the effects of IR on the cytoskeleton. However, therapeutic doses of irradiation were shown to affect cell permeability of microvascular endothelial cells through Rho-mediated cytoskeleton remodeling (37). More recently, Rho-mediated focal adhesion and fibronectin adhesion were shown to be increased in endothelial cells in response to radiation (38). As Rho GTPases intervene in a number of additional cell pathways (e.g., cell cycle arrest, and regulation of apoptosis) (39), Rho GTPases potentially play a pivotal role in the cell response to simulated space conditions. In agreement with this hypothesis, GSEA revealed that Rho GTPases activity was downregulated in IR-treated samples. Notably, gene sets involved in integrin and receptor binding were specifically downregulated following treatment using the RPM. The results of this study confirm therefore

that integrins play a significant role in the cellular response to simulated microgravity.

In conclusion, this study has shown that continuous exposure to simulated microgravity affects fetal murine fibroblasts, especially at the single gene level, by increasing the expression of oxidative stress responsive genes and decreasing the expression of genes involved in cytoskeleton remodeling. As far as irradiation is concerned, we detected a decreased expression of gene sets involved in cytoskeleton mechanisms, in cell signaling and DNA damage response after a chronic low-dose rate of irradiation, particularly at the gene set level. The results indicate that the effects of the combination of the two treatments did not result in a synergism between the two separate effects, since many genes or gene sets that were altered by RPM or IR treatment, were not changed by the combined treatment (RPM and IR).

### Acknowledgements

This study was supported by the ESA Topical Team on 'Developmental Biology in Vertebrates' and 4 PRODEX/ESA contracts [C90-303, C90-380, C90-391 and 42-000-90-380].

### References

- Huijser RH: Desktop RPM: new small size microgravity simulator for the bioscience laboratory. *Fokker Space FS-MG-R00-017*: 1-5, 2000.
- van Loon JJWA: Some history and use of the random positioning machine, RPM, in gravity related research. *Adv Space Res* 39: 1161-1165, 2007.
- Borst A and van Loon J: Technology and developments for the random positioning machine, RPM. *Microgravity Sci Technol* 21: 287-292, 2009.
- Kraft TF, van Loon JJ and Kiss JZ: Plastid position in arabidopsis columella cells is similar in microgravity and on a random-positioning machine. *Planta* 211: 415-422, 2000.
- Villa A, Versari S, Maier JA and Bradamante S: Cell behavior in simulated microgravity: a comparison of results obtained with RWV and RPM. *Gravit Space Biol Bull* 18: 89-90, 2005.
- Grimm D, Bauer J, Ulbrich C, *et al*: Different responsiveness of endothelial cells to vascular endothelial growth factor and basic fibroblast growth factor added to culture media under gravity and simulated microgravity. *Tissue Eng Part A* 16: 1559-1573, 2010.
- Mastroleo F, Van Houdt R, Leroy B, *et al*: Experimental design and environmental parameters affect *Rhodospirillum rubrum* SIH response to space flight. *ISME J* 3: 1402-1419, 2009.
- Shi J and Walker MG: Gene set enrichment analysis (GSEA) for interpreting gene expression profiles. *Curr Bioinform* 2: 133-137, 2007.
- Subramanian A, Tamayo P, Mootha VK, *et al*: Gene set enrichment analysis: A knowledge-based approach for interpreting genome-wide expression profiles. *Proc Natl Acad Sci USA* 102: 15545-15550, 2005.
- El-Saghire H, Thierens H, Monsieurs P, Michaux A, Vandevoorde C and Baatout S: Gene set enrichment analysis highlights different gene expression profiles in whole blood samples X-irradiated with low and high doses. *Int J Radiat Biol* 89: 628-638, 2013.
- Vanhavere F, Loos M, Plompen AJM, Wattecamps E and Thierens H: A combined use of the BD-PND and BDT bubble detectors in neutron dosimetry. *Radiat Meas* 29: 573-577, 1998.
- Cucinotta FA, Kim MH, Willingham V and George KA: Physical and biological organ dosimetry analysis for international space station astronauts. *Radiat Res* 170: 127-138, 2008.
- Crawford-Young SJ: Effects of microgravity on cell cytoskeleton and embryogenesis. *Int J Dev Biol* 50: 183-191, 2006.
- Meloni MA, Galleri G, Pani G, Saba A, Pippia P and Cogoli-Greuter M: Space flight affects motility and cytoskeletal structures in human monocyte cell line J-111. *Cytoskeleton (Hoboken)* 68: 125-137, 2011.
- Hayes JD and McLellan LI: Glutathione and glutathione-dependent enzymes represent a co-ordinately regulated defence against oxidative stress. *Free Radic Res* 31: 273-300, 1999.
- Chen Y, Johansson E, Fan Y, *et al*: Early onset senescence occurs when fibroblasts lack the glutamate-cysteine ligase modifier subunit. *Free Radic Biol Med* 47: 410-418, 2009.
- Haines DD, Lekli I, Teissier P, Bak I and Tosaki A: Role of haeme oxygenase-1 in resolution of oxidative stress-related pathologies: Focus on cardiovascular, lung, neurologic and kidney disorders. *Acta Physiol (Oxf)* 204: 487-501, 2012.
- Lee JC, Kinniry PA, Arguiri E, *et al*: Dietary curcumin increases antioxidant defenses in lung, ameliorates radiation-induced pulmonary fibrosis, and improves survival in mice. *Radiat Res* 173: 590-601, 2010.
- Hayes JD and McMahon M: NRF2 and KEAP1 mutations: permanent activation of an adaptive response in cancer. *Trends Biochem Sci* 34: 176-188, 2009.
- Wang J, Zhang J, Bai S, *et al*: Simulated microgravity promotes cellular senescence via oxidant stress in rat PC12 cells. *Neurochem Int* 55: 710-716, 2009.
- Nikawa T, Ishidoh K, Hirasaka K, *et al*: Skeletal muscle gene expression in space-flown rats. *FASEB J* 18: 522-524, 2004.
- Liu Y and Wang E: Transcriptional analysis of normal human fibroblast responses to microgravity stress. *Genomics Proteomics Bioinformatics* 6: 29-41, 2008.
- Carson JA, Culbertson DE, Thompson RW, Fillmore RA and Zimmer W: Smooth muscle gamma-actin promoter regulation by RhoA and serum response factor signaling. *Biochim Biophys Acta* 1628: 133-139, 2003.
- Philippart U, Schratz G, Dieterich C, *et al*: The SRF target gene *Fhl2* antagonizes RhoA/MAL-dependent activation of SRF. *Mol Cell* 16: 867-880, 2004.
- Beamish JA, He P, Kottke-Marchant K and Marchant RE: Molecular regulation of contractile smooth muscle cell phenotype: implications for vascular tissue engineering. *Tissue Eng Part B Rev* 16: 467-491, 2010.
- Olson EN and Nordheim A: Linking actin dynamics and gene transcription to drive cellular motile functions. *Nat Rev Mol Cell Biol* 11: 353-365, 2010.
- Sun Q, Chen G, Streb JW, *et al*: Defining the mammalian CARome. *Genome Res* 16: 197-207, 2006.
- Ingber DE: Tensegrity II. How structural networks influence cellular information processing networks. *J Cell Sci* 116: 1397-1408, 2003.
- Meloni MA, Galleri G, Pippia P and Cogoli-Greuter M: Cytoskeleton changes and impaired motility of monocytes at modelled low gravity. *Protoplasma* 229: 243-249, 2006.
- Servotte S, Zhang Z, Lambert CA, *et al*: Establishment of stable human fibroblast cell lines constitutively expressing active rho-GTPases. *Protoplasma* 229: 215-220, 2006.
- Nichols HL, Zhang N and Wen X: Proteomics and genomics of microgravity. *Physiol Genomics* 26: 163-171, 2006.
- Loesberg WA, Walboomers XF, van Loon JJWA and Jansen JA: Simulated microgravity activates MAPK pathways in fibroblasts cultured on microgrooved surface topography. *Cell Motil Cytoskeleton* 65: 116-129, 2008.
- Hall A: Rho GTPases and the control of cell behaviour. *Biochem Soc Trans* 33: 891-895, 2005.
- Jeggo P: The role of the DNA damage response mechanisms after low-dose radiation exposure and a consideration of potentially sensitive individuals. *Radiat Res* 174: 825-832, 2010.
- Jeggo P and Lavin MF: Cellular radiosensitivity: how much better do we understand it? *Int J Radiat Biol* 85: 1061-1081, 2009.
- Grimm D, Wise P, Lebert M, Richter P and Baatout S: How and why does the proteome respond to microgravity? *Expert Rev Proteomics* 8: 13-27, 2011.
- Gabryś , Greco O, Patel G, Prise KM, Tozer GM and Kanthou C: Radiation effects on the cytoskeleton of endothelial cells and endothelial monolayer permeability. *Int J Radiat Oncol Biol Phys* 69: 1553-1562, 2007.
- Rousseau M, Gaugler MH, Rodallec A, Bonnaud S, Paris F and Corre I: RhoA GTPase regulates radiation-induced alterations in endothelial cell adhesion and migration. *Biochem Biophys Res Commun* 414: 750-755, 2011.
- Etienne-Manneville S and Hall A: Rho GTPases in cell biology. *Nature* 420: 629-635, 2002.